



Stalagmite-inferred abrupt climate change of Asian Summer Monsoon at MIS 5a/4 transition

Xiuyang Jiang ^{1,2*}, Yaoqi He ³, Xiaoyan Wang ¹, Jinguo Dong ⁴, Zhizhong Li ^{1,2}, Chuan-Chou Shen ^{5*}

5

¹ Key Laboratory of Humid Subtropical Eco-geographical Processes, Ministry of Education, College of Geography Science, Fujian Normal University, Fuzhou 350007, China

² Institute of Geography, Fujian Normal University, Fuzhou 350007, China

³ College of Tourism and Air Service, Guizhou Minzu University, Guiyang 550025, China

10 ⁴ College of Geosciences, Nantong University, Nantong 226007, China

⁵ High-Precision Mass Spectrometry and Environment Change Laboratory (HISPEC), Department of Geosciences, National Taiwan University, Taipei 106, Taiwan ROC

15 *Correspondence to: Xiuyang Jiang (xyjiang@fjnu.edu.cn) and Chuan-Chou Shen (river@ntu.edu.tw)



Abstract

The Greenland Interstadial 21 (GIS 21), one of the longest warm events during the last glacial, occurred in conjunction with the transition from marine isotope stages (MIS) 5a to 4. Precise determination of the timing and duration of this event can improve our understanding of hydroclimatic connection between low and high latitudes over this MIS boundary. Facilitated by a robust chronology with closely spaced U-Th ages, replicated sub-decadal-resolved $\delta^{18}\text{O}$ records of two stalagmites from Sanxing Cave, Southwest China, express Asian Summer Monsoon (ASM) history from 79.0 ± 0.2 to 75.7 ± 0.2 thousand years before present (kyr BP, before AD 1950) to reveal detailed structure of MIS 5a/4 transition and Chinese Interstadial (CIS) 21. The composited Sanxing record is characterized with three centennial-scale strong monsoon peaks and a 700-yr-long weak monsoon period within the CIS 21 “rebound-type” event, concurrent with its counterpart of Greenland Interstadial 21 (GIS 21). This strong resemblance suggests a rapid atmospheric teleconnection between the North Atlantic and the ASM regions. The transition at the termination of the Chinese Interstadial (CIS) 21 is determined to be from 77.0 ± 0.2 to 76.6 ± 0.2 kyr BP with a mid-point at 76.8 ± 0.2 kyr BP, which is 0.5-1.0 kyr younger than the correspondent of the end of GIS 21 on GICC05modelext and AICC2012 timescales. Given its high accuracy, our Sanxing Cave chronology can become one of the potential references for chronological refinement for ice-core records.

Keywords: *Asian summer monsoon, Stalagmite, Sanxing Cave, MIS 5a/4 transition, CIS 21*



1 Introduction

Millennial-scale abrupt climate oscillations known as Dansgaard-Oeschger (D-O) events, referred to as relatively warm Greenland interstadials (GISs) and cold Greenland stadials (GSs), during the last glacial were first revealed from ice cores of Camp Century in Greenland by Johnsen et al. (1972). Over the studies in the past decades, these D-O events have been documented in global proxy records, including bipolar ice cores (e.g., Dansgaard et al., 1993; North Greenland Ice Core Project members, 2004; EPICA Community Members, 2006; WAIS Divide Project Members, 2015), deep-sea sediments (Bond et al., 1993; McManus et al., 1999; Deplazes et al., 2013), loess (Porter and An., 1995; Sun et al., 2011), lacustrine sediments (Tierney et al., 2008), and speleothems (e.g., Wang et al., 2001; Genty et al., 2003; Spötl et al., 2006; Chen et al., 2016).

In 2001, Hulu cave stalagmite $\delta^{18}\text{O}$ record first showed the predominant influence of these high-latitude climate oscillations on Asian summer monsoon intensity via reorganization of atmosphere circulation (Wang et al., 2001). The advanced understanding of this teleconnection was established by subsequent studies (e.g., Cai et al., 2006; Liu et al., 2010; Zhao et al., 2010; Zhou et al., 2011; Duan et al., 2014; Chen et al., 2016; Duan et al., 2016; Zhang et al., 2017), mainly covering marine isotope stages (MIS) 4-2. Our knowledge of millennial-scale abrupt climatic evolution before MIS 4 is, however, limited by records with multidecadal resolution and large dating uncertainties of several hundreds of years (Wang et al., 2008).

Comparing to MIS 4-2, MIS 5d-5a [(110–74 thousand years ago (kyr BP, relative to AD 1950)], including the last glacial inception and the early glacial (Shackleton, 1987), is characterized with higher atmospheric CO_2 (Petit et al., 1999), and a different orbital configuration with stronger eccentricity



and larger seasonal insolation changes (Berger, 1991). The long millennial GIS events, 25-21, during the period were, therefore, less frequent compared to those at MIS 4-2 (North Greenland Ice Core Project members, 2004; Capron et al., 2010a). NGRIP ice-core record (Capron et al., 2010b) expressed that the longest and warmest GIS 21 is featured with a clearly sub-millennial “rebound-type” event before its termination. This rapid cooling at the end of GIS 21 at 77 kyr BP marks the transition from warm MIS 5a interstadial to cold MIS 4 stadial. Precise determination of the timing and duration of GIS 21 can help to understand global climate correlations across the MIS 5a/4 boundary.

Here, we report two new replicated sub-decadal-resolved stalagmites records with precision as good as ± 200 yr from southwestern China to reveal a detailed Asian summer monsoon (ASM) history at Chinese Interstadial (CIS, Cheng et al., 2006) 21 from 79.0-75.7 kyr BP. Comparison with Greenland ice core records reveals concurrent hydroclimatic dynamics on centennial-millennial timescales over the GIS 21 from MIS 5a-4 at both low and high latitudes.

2 Locations, materials and methods

Sanxing Cave (27°22'N, 107°11'E, 720 m above sea level) is located in Tiechang town, 80 km southeast to Zuiyi City, Guizhou Province, Southwest China (Fig. 1). This 2 km-long cave, with only one entrance, is 600 km southwest from Sanbao and Yongxing caves, Central China (Wang et al., 2008; Chen et al., 2016). The regional climate experiences typical subtropical monsoon and is characterized with distinct seasons, rainy in hot summer and dry in cold winter. Local temperature ranges from 1.6 °C in winter and 22.5 °C in summer and annual mean temperature is 13.5 °C recorded at the nearest meteorological station in Zuiyi City from AD 1950-2000. Mean annual precipitation is 980 ± 50 mm



(1 σ ; AD 1950-2000). The cave is overlain by 30 m-thick Permian limestone with a thin soil cover. The well-developed vegetation consists mainly of subtropical broadleaf evergreen and deciduous mixed forests.

Two calcite stalagmites, SX10 and SX16 (Fig. 2), 1016 mm and 431 mm in length respectively, were collected in a chamber 900 m from the entrance. SX10 was broken into four segments when collecting. SX16 was partially buried under clay-rich silt. Stalagmites were halved using a diamond saw. They are pure calcite with typical coalescent columnar-fabric crystals and no any visible porous defect on the polished surface are observed (Fig. 2). For stalagmite SX10, one clay band can be observed at the depth of 817-820 mm from top (Fig. 2), suggesting a possible growth discontinuity. One brown detrital lamina on stalagmite SX16 can be found at 290 mm from top (Fig. 2).

Twenty subsamples, sixteen from SX10 and four from SX16, were dated with U-Th dating methods. About 60 mg of powdered subsample was drilled from the polished surface using a 0.9 mm diameter carbide dental drill on a class-100 clean bench in a class-10,000 clean sampling room to avoid possible contamination. Procedure for chemical separation and purification of uranium and thorium was described in Shen et al. (2003). U-Th isotopic compositions and concentrations were determined on a Thermo-Fisher NEPTUNE multi-collection inductively coupled plasma mass spectrometer (MC-ICP-MS) at the High-Precision Mass Spectrometry and Environment Change Laboratory (HISPEC), Department of Geosciences, National Taiwan University (Shen et al., 2012). Half-lives of U-Th nuclides used are listed in Cheng et al. (2013). Uncertainties in the U-Th isotopic data and ^{230}Th dates (yr BP), relative to 1950 AD, are given at the two-sigma (2σ) level or two standard deviations of the mean ($2\sigma_m$) unless otherwise noted.



For $\delta^{18}\text{O}$ measurement, subsamples, 100 μg each, were milled at 2-mm intervals along central growth axis using a 0.5-mm carbide dental burr. A total of 566 powdered subsamples were analyzed on a Finnigan MAT-253 mass spectrometer connected to an on-line automated preparation system (Gasbench II) at the College of Geography Science, Fujian Normal University. Results were reported relative to the Vienna Pee Dee Belemnite (VPDB) standard and standardization was accomplished using NBS-19. Precision of $\delta^{18}\text{O}$ values is $\pm 0.1\text{‰}$ at 2σ level.

3 Results

3.1 Chronology

U-Th isotopic compositions and ^{230}Th dates are given in Table 1. For stalagmite SX10, High ^{238}U content ($[^{238}\text{U}]$) is 1.4-2.0 ppm and low $[^{232}\text{Th}]$ ranges from 86-725 ppt. High $^{230}\text{Th}/^{232}\text{Th}$ atomic ratios range from 70 to 649×10^{-3} , indicative of minimal detrital thorium contamination. Uncertainties of corrected ^{230}Th dates are from ± 153 to ± 213 yr (Table 1). For stalagmite SX16, $[^{238}\text{U}]$ is 0.5-1.7 ppm and $[^{232}\text{Th}]$ ranges from 653-2281 ppt. ^{230}Th dates are measured with a precision of ± 216 -321 yr (Table 1).

All ^{230}Th dates are in stratigraphic order (Table 1). Two hiatuses at the depth of 817-820 mm of SX10 and 290 mm of SX16, are respectively bounded with dates of 78.3 and 78.7 kyr BP, and 68.8 and 75.8 kyr BP. ^{230}Th dates reveal that stalagmite SX10, with growth rates of 0.7-5.9 yr/mm, deposited from 78.9 to 75.7 kyr BP (Table 1). The lower part of SX16 formed from 77.0 to 75.8 kyr BP with deposition rates of 9.4-16.7 yr/mm. The upper segment of SX16, with ages < 69 kyr BP, was not used in this study.

A linear interpolation between ^{230}Th dates and an algorithm method, called “StalAge” (Scholz and



Hoffmann, 2011), were used to establish age models. The age-depth relations are plotted in Figure 3. The results show no significant difference between two chronologies (Fig. 3). In order to directly compare with previous caves studies (Wang et al., 2008; Chen et al., 2016), we choose the same (i.e. linear interpolation) method to build age models of SX10 and SX16.

5

3.2 Oxygen isotope record

The 7-year resolved Sanxing Cave stalagmite $\delta^{18}\text{O}$ profiles are shown in Figure 4. The replication test (Dorale and Liu, 2009) between two Sanxing Cave stalagmites, SX10 and SX16, expresses synchronous variations for the contemporaneous $\delta^{18}\text{O}$ records from 77.1 to 75.8 kyr BP (Fig. 4), suggesting that the stalagmite deposited at an oxygen isotopic equilibrium condition and can register regional hydroclimate change. As previously suggested by proxy records and simulated models (e.g., Wang et al., 2001, 2008; Yuan et al., 2004; Cheng et al., 2009, 2016; Liu et al., 2010; Duan et al., 2014; Zhang et al., 2014; Liu et al., 2014; Dong et al., 2015; Jiang et al., 2016; Chen et al., 2016), Chinese stalagmite $\delta^{18}\text{O}$ time series mainly represent ASM evolution.

15 The $\delta^{18}\text{O}$ values vary from -9.7 to -6.0‰ throughout the whole Sanxing Cave record with decadal- to centennial-scale events. The duration from 79.0 to 77.0 kyr BP is characterized with the lowest $\delta^{18}\text{O}$ data, fluctuating between -9.5 and -7.5‰ with a mean average value of -8.9‰. After 77.0 kyr BP, Sanxing record shows an abrupt 400-yr $\delta^{18}\text{O}$ increase of 2.0‰, indicating a major climatic shift from MIS 5a interstadial to MIS 4 stadial (Fig. 4), followed by a slow $\delta^{18}\text{O}$ increasing to -7.1‰ from 76.6 to
20 75.7 kyr BP.



4 Discussion

4.1 The end of CIS 21

Sanxing stalagmite $\delta^{18}\text{O}$ sequence captures the detailed process of ASM dynamics at the end of CIS 21. The chronology from 77.0 to 76.6 kyr BP for SX10 oxygen isotope record is tightly anchored by four
5 high-precision ^{230}Th ages with an averaged 2σ error of ± 0.2 kyr (Fig. 4). The beginning and termination of the sharp 400-yr transition of CIS termination are respectively calendared with two dates of 77.0 ± 0.2 and 76.6 ± 0.2 kyr BP (vertical bar in Fig. 4), supported by a statistical regression approach RAMPFIT (Mudelsee, 2000) (Fig. 4). The mid-point of this transition, considered as the termination of
10 CIS 21, in SX10 record is determined at 76.8 kyr BP with an uncertainty of ± 0.2 kyr, more precise than those in caves of Sanbao (77.1 ± 0.7 kyr BP; Wang et al., 2008) and Yongxing (76.5 ± 0.4 kyr BP; Chen et al., 2016) (Fig. 5).

4.2 CIS 21 rebound event

The NGRIP $\delta^{18}\text{O}$ profile shows a 1.2 yr-long warming interval (Fig. 6), referred to as a rebound-type
15 event (Capron et al., 2010a), at the end of GIS 21 and before entering a cold stadial. This event is also observed in a multi-annually resolved low-latitude marine sediment record from Cariaco Basin on the northern shelf of Venezuela (Deplazes et al., 2013). It, however, is not clearly expressed in previous Chinese stalagmite records (Xia et al., 2007; Wang et al., 2008; Chen et al., 2016), most likely limited to their temporal resolution.

20 Our new Sanxing record clearly registers this rebound event from 78.4 to 77.2 kyr BP (Fig. 6). In Sanxing $\delta^{18}\text{O}$ record, it can be divided with two distinct stages: a strong monsoon interval at 78.4-77.8



kyr BP and a weak one between 77.8-77.2 kyr BP. The 0.6-kyr strong monsoon period is featured with three centennial-scale events (labeled as **a**, **b**, and **c** in Fig. 6), matching the equivalent warming peaks in Greenland. Our Sanxing record also shows a 700-yr-long weak monsoon interval, with a sharp 0.8‰ enrichment excursion in $\delta^{18}\text{O}$, centered at 77.4 kyr BP, strongly resembling its counterpart in Greenland (Fig. 6). The first-time identification of CIS 21 rebound monsoonal event in a low-latitude continental archive indicates a large-scale climatic footprint of the NH high latitudes on the ASM realm.

The striking similarity of centennial-scale variability between Greenland ice core and Chinese stalagmite records is not only visible during the boundary of MIS 5a/4, but also during the MIS 5 (Jiang et al., 2016), early MIS 3 (Liu et al., 2010; Duan et al., 2016), MIS 3/2 (Zhao et al., 2010), and last glacial maximum (Duan et al., 2015). The close coupling of abrupt centennial-millennial climatic oscillations, one of persistent features during the last glacial, between AM territory and Greenland suggests that atmospheric circulation changes are important in transmitting abrupt climatic signals from high- to low-latitude realms (Liu et al., 2010; Zhao et al., 2010; Duan et al., 2016). The westerlies could be the critical bridge to transmit abrupt climatic signals to the ASM (Porter and An, 1995; Nagashima et al., 2011, Chiang et al., 2015; Duan et al., 2016).

4.3 Absolute age control for MIS 5a/4 transition

Absolute ^{230}Th dated stalagmite $\delta^{18}\text{O}$ record from Hulu Cave, China, firstly shown a series millennial-scale ASM peaks between 75-11 kyr BP (Wang et al., 2001), which correspondingly match GIS (GS) events recorded in Greenland ice cores. After significant discrepancies between Hulu and GRIP/GISP2 time scales at 20 kyr BP were revealed in the study by Wang et al. (2001), refinements of



Greenland ice core age models were continuously refined (e.g. Genty et al., 2003; Cruz et al., 2005; Spöhl et al., 2006). Even the most robust multi-parameter and annual layer-counted GICC05 timescale (Svensson et al., 2008) is, however, associated with uncertainties up to 2.6 ka at ages >60 ka (Wolff et al., 2010).

5 Recently, an integrated ^{230}Th -dated stalagmite $\delta^{18}\text{O}$ record at 120-60 kyr BP from the northern rim of the Alps (NALPS) (Boch et al., 2011) and our previously published ^{230}Th -dated Sanxing Cave stalagmite $\delta^{18}\text{O}$ record at 113.-86.6 kyr BP (Jiang et al., 2016) provided a promising reference for Greenland ice cores records. Our new Sanxing records covering from 79.0 ± 0.2 to 75.7 ± 0.2 kyr BP offer additional age references for chronological calibration of bipolar ice cores at the transition of MIS
10 5a/4.

In Figure 6, the Sanxing stalagmite $\delta^{18}\text{O}$ record is compared with NGRIP $\delta^{18}\text{O}$ records on the GICC05modelext (Wolff et al., 2010) and AICC2012 timescales (Veres et al., 2013) from 79.0 to 75.7 kyr BP. The termination of GIS 21 is constrained at 77.8 kyr BP and 77.3 kyr BP with age models of GICC05modelext and AICC2012, respectively, which is 0.5-1.0 kyr older than the correspondent in
15 Sanxing cave records (Fig. 6). Even the offsets are within the age uncertainties of >2.6 kyr of the GICC05modelext and AICC2012 timescales for the MIS 5a/4, our well-dated Sanxing record can be used to improve the accuracy of Greenland ice-core chronologies.

5 Conclusions

20 With high-precision ^{230}Th ages and over 500 oxygen isotope data, two stalagmites from Sanxing Cave in northern Guizhou Province, Southwest China, reveal regional ASM history from 79.0 ± 0.2 to



75.7±0.2 kyr BP. The well-dated sub-decadal-resolved stalagmite-inferred CIS 21 rebound event suggests a large-scale climatic footprint of the NH high latitudes on the ASM. The decreasing ASM transition at the termination of the CIS 21, from 77.0±0.2 to 76.6±0.2 kyr BP with a mid-point at 76.8±0.2 kyr BP, can be used for chronological calibration of different proxy records.

5

Contribute. X.J. designed research; X.J. and Y.H. collected the stalagmites; X.W., J. D., and C.S. were responsible for ²³⁰Th dating; X.W. performed oxygen isotope analysis; X.J and C.S. prepared the draft and all author contributed towards preparing the manuscript.

10 **Competing interests.**

The authors declare that they have no conflict of interest.

Acknowledgments. This study was jointly supported by grants of the National Natural Science Foundation of China (41372189, 41672170), Natural Science Foundation of Fujian Province (2017J01654), and the Outstanding Youth Scientific Research Program in Fujian Province University. Funding was also provided by grants from Taiwan ROC MOST (104-2119-M-002-003, 105-2119-M-002-001 to C.-C.S.) and the National Taiwan University (105R7625 to C.-C.S.).

References

- 20 Berger, A. and Loutre, M.F.: Insolation values for the climate of the last 10 million years, *Quat. Sci. Rev.*, 10, 297-317, 1991.
- Boch, R., Cheng, H., Spötl, C., Edwards, R.L., Wang, X., and H äuselmann, P.: NALPS: A precisely dated European



- climate record 120-60 ka, *Clim. Past.*, 7, 1247-1259, 2011.
- Bond, G., Broecker, W., Johnsen, S., McManus, J., Labeyrie, L., Jouzel, J., and Bonani, G.: Correlations between climate records from North Atlantic sediments and Greenland ice, *Nature*, 365, 143-147, 1993.
- Cai, Y., An, Z., Cheng, H., Edwards, R.L., Kelly, M.J., Liu, W., Wang, X., and Shen, C.-C.: High-resolution absolute-dated Indian monsoon record between 53 and 36 ka from Xiaobailong Cave, southwestern China, *Geology*, 34, 621-624, 2006.
- 5 Capron, E., Landais, A., Chappellaz, J., Schilt, A., Buiron, D., Dahl-Jensen, D., Johnsen, S.J., Jouzel, J., Lemieux-Dudon, B., Louergue, L., Leuenberger, M., Masson-Delmotte, V., Meyer, H., Oerter, H., and Stenni, B.: Millennial and sub-millennial scale climatic variations recorded in polar ice cores over the last glacial period, *Clim. Past.*, 6, 345-365, 2010a.
- 10 Capron, E., Landais, A., Lemieux-Dudon, B., Schilt, A., Masson-Delmotte, V., Buiron, D., Chappellaz, J., Dahl-Jensen, D., Johnsen, S.J., Leuenberger, M., Louergue, L., and Oerter, H.: Synchronising EDML and NorthGRIP ice cores using $\delta^{18}\text{O}$ of atmospheric oxygen ($\delta^{18}\text{O}_{\text{atm}}$) and CH_4 measurements over MIS 5 (80-123 kyr), *Quat. Sci. Rev.*, 29, 222-234, 2010b.
- 15 Chiang, J.C.H., Fung, I.Y., Wu, C.H., Cai Y.J., Edman, J.P., Liu, Y.W., Day, J.A., Bhattacharya, T., Mondal, Y., and Labrousse, C.A.: Role of seasonal transitions and westerly jets in East Asian paleoclimate, *Quat. Sci. Rev.*, 108, 111-129, 2015.
- Chen, S.T., Wang, Y.J., Cheng, H., Edwards, R.L., Wang, X.F., Kong, X.G., and Liu, D.B.: Strong coupling of Asian Monsoon and Antarctic climates on sub-orbital timescales, *Sci. Rep.*, 6, 32995, doi: 10.1038/srep32995, 2016.
- 20 Cheng, H., Edwards, R.L., Kong, X.G., Ming, Y.F., Kelly, M.J., Wang, X.F., Gallup, C.D., and Liu, W.G.: A penultimate glacial monsoon record from Hulu Cave and two-phase glacial terminations, *Geology*, 34, 217-220, 2006.
- Cheng, H., Edwards, R.L., Broecker, W.S., Denton, G.H., Kong, X., Wang, Y., Zhang, R., and Wang, X.: Ice age terminations, *Science*, 326, 248-252, 2009.
- Cheng, H., Edwards, R.L., Shen, C.-C., Polyak, V.J., Asmerom, Y., and Woodhead, J.: Improvements in ^{230}Th dating, ^{230}Th and ^{234}U half-life values, and U-Th isotopic measurements by multi-collector inductively coupled plasma mass spectrometry, *Earth. Planet. Sci. Lett.*, 371-372, 82-91, 2013.
- 25 Cheng, H., Edwards, R.L., Sinha, A., Spöhl, C., Yi, L., Chen, S.T., Kelly, M., Kathayat, G., Wang, X.F., Li, X.L., Kong, X.G., Wang, Y.J., Ning, Y.F., and Zhang, H.W.: The Asian monsoon over the past 640,000 years and ice age terminations, *Nature*, 534, 640-646, 2016.
- 30 Cruz, F.W., Karmann, I., Viana, O.J., Burns, S.J., Ferrari, J.A., Vuille, M., Sial, A.N., and Moreira, M.Z.: Stable isotope study of cave percolation waters in subtropical Brazil: Implications for paleoclimate inferences from speleothems, *Chem. Geol.*, 220, 245-262, 2005.



- Dansgaard, W., Johnsen, S.J., Clausen, H.B., Dahl-Jensen, D., Gunderstrup, N.S., Hammer, C.U., Steffensen, J.P., Sveinbjörnsdóttir, A., Jouzel, J., and Bond, G.: Evidence for general instability of past climate from a 250-kyr ice-core record, *Nature*, 364, 218-220, 1993.
- Deplazes, G., Lückge, A., Peterson, L.C., Timmermann, A., Hamann, Y., Hughen, K.A., Röhl, U., Laj, C., Cane, M.A., Sigman, D.M., and Haug, G.H.: Links between tropical rainfall and North Atlantic climate during the last glacial period, *Nat. Geosci.*, 6, 213-217, 2013.
- Dong, J.G., Shen, C.-C., Kong, X.G., Wang, H.-C., and Jiang, X.Y.: Reconciliation of hydroclimate sequences from the Chinese Loess Plateau and low-latitude East Asian Summer Monsoon regions over the past 14,500 years, *Palaeogeogr. Palaeoclimatol. Palaeoecol.*, 435, 127-135, 2015.
- Dorale, J.A. and Liu, Z.: Limitations of Hendy test criteria in judging the paleoclimate suitability of speleothems and the need for replication, *J. Cave. Karst. Stud.*, 71, 73-38, 2009.
- Duan, F., Liu, D., Cheng, H., Wang, X., Wang, Y., Kong, X., and Chen, S.: A high resolution monsoon record of millennial-scale oscillations during Late MIS 3 from Wulu Cave, south-west China, *J. Quat. Sci.*, 29, 83-90, 2014.
- Duan, F., Wu, J., Wang, Y., Edwards, R., Cheng, H., Kong, X., and Zhang, W.: A 3000-yr annually laminated stalagmite record of the Last Glacial Maximum from Hulu Cave, China, *Quat. Res.*, 83, 360-369, 2015.
- Duan, W.H., Cheng, H., Tan, M., and Edwards, R.L.: Onset and duration of transitions into Greenland Interstadials 15.2 and 14 in northern China constrained by an annually laminated stalagmite, *Sci. Rep.*, 6, 20844, doi: 10.1038/srep20844, 2016.
- EPICA Community Members.: One to one coupling of glacial climate variability in Greenland and Antarctica, *Nature*, 444, 195-198, 2006.
- Genty, D., Blamart, D., Ouahdi, R., Gilmour, M., Baker, A., Jouzel, J., and Van-Exter, S.: Precise dating of Dansgaard-Oeschger climate oscillations in western Europe from stalagmite data, *Nature*, 421, 833-837, 2003.
- Jiang, X.Y., Wang, X.Y., He, Y.Q., Hu, H.-M., Li, Z.Z., Spötl, C., and Shen, C.-C.: Precisely dated multidecadally resolved Asian summer monsoon dynamics 113.5-86.6 thousand years ago, *Quat. Sci. Rev.*, 143, 1-12, 2016.
- Johnsen, S.J., Dansgaard, W., Clausen, H.B., and Langway, C.C.: Oxygen isotope profiles through the antarctic and greenland ice sheets, *Nature*, 235, 429-434, 1972.
- Liu, D., Wang, Y., Cheng, H., Edwards, R.L., Kong, X., Wang, X., Hardt, B., Wu, J., Chen, S., Jiang, X., He, Y., Dong, J., and Zhao, K.: Sub-millennial variability of Asian monsoon intensity during the early MIS 3 and its analogue to the ice age terminations, *Quat. Sci. Rev.*, 29, 1107-1115, 2010.
- Liu, Z., Wen, X., Brady, E.C., Otto-Bliesner, B., Yu, G., Lu, H., Cheng, H., Wang, Y., Zheng, W., Ding, Y., Edwards, R.L., Cheng, J., Liu, W., and Yang, H.: Chinese cave records and the East Asia Summer Monsoon, *Quat. Sci. Rev.*, 83, 115-128, 2014.



- McManus, J.F., Oppo, D.W., and Cullen, J.L.: A 0.5-million-year record of millennial-scale climate variability in the North Atlantic, *Science*, 283, 971-975, 1999.
- Mudelsee, M.: Ramp function regression: A tool for quantifying climate transitions, *Comput. Geosci.*, 26, 293-307, 2000.
- 5 Nagashima, K., Tada, R., and Tani, A.: Millennial-scale oscillations of the westerly jet path during the last glacial period, *J. Asian. Earth. Sci.*, 40, 1214-1220, 2011.
- North Greenland Ice Core Project Members.: High-resolution record of Northern Hemisphere climate extending into the last interglacial period, *Nature*. 431, 147-151, 2004.
- Petit, J.R., Jouzel, J., Raynaud, D., Barkov, N.L., Barnola, J.-M., Basile, L., Bender, M., Chappellaz, J., Davis, M.,
10 Delaygue, G., Delmotte, M., Kotlyakov, V. M., Legrand, M., Lipenkov, V.Y., Lorius, C., P \acute{e} pin, L., Ritz, C., Saltzman, E., and Stievenard, M.: Climate and atmospheric history of the past 420,000 years from the Vostok ice core, Antarctica, *Nature*, 399, 429-436, 1999.
- Porter, S.C. and An, Z.S.: Correlation between climate events in the North Atlantic and China during the last glaciation, *Nature*, 375, 305-308, 1995.
- 15 Scholz, D. and Hoffmann, D.L.: StalAge-an algorithm designed for construction of speleothem age models, *Quat. Geochronol.*, 6, 369-382, 2011.
- Shackleton, N.J.: Oxygen isotopes, ice volume and sea level, *Quat. Sci. Rev.*, 6, 183-190, 1987.
- Shen, C.-C., Cheng, H., and Edwards, R.L.: Measurement of attogram quantities of ^{231}Pa in dissolved and particulate fractions of seawater by isotope dilution thermal ionization mass spectroscopy, *Anal. Chem.*, 75, 1075-1079, 2003.
- 20 Shen, C.-C., Wu, C.-C., Cheng, H., Edwards, R.L., Hsieh, Y.-T., Gallet, S., Chang, C.-C., Li, T., Lam, D.D., Kano, A., Hori, M., and Sp \ddot{a} tl, C.: High-precision and high-resolution carbonate ^{230}Th dating by MC-ICP-MS with SEM protocols, *Geochim. Cosmochim. Acta.*, 99, 71-86, 2012.
- Sp \ddot{a} tl, C., Mangini, A., and Richards, D.A.: Chronology and paleoenvironment of Marine Isotope Stages 3 from two high-elevation speleothems, Austrian Alps, *Quat. Sci. Rev.*, 25, 1127-1136, 2006.
- 25 Sun, Y.B., Clemens, S.C., Morrill, C., Lin, X.P., Wang, X.L., and An, Z.S.: Influence of Atlantic meridional overturning circulation on the East Asian winter monsoon, *Nat. Geosci.*, 5, 46-49, 2012.
- Svensson, A., Andersen, K.K., Bigler, M., Clausen, H.B., Dahl-Jensen, D., Davies, S.M., Johnsen, S.J., Muscheler, R., Parrenin, F., Rasmussen, S.O., R \ddot{a} thlisberger, R., Seierstad, I., Steffensen, J.P., and Vinther, B.M.: A 60,000 year Greenland stratigraphic ice core chronology, *Clim. Past.*, 4, 47-57, 2008.
- 30 Tierney, J.E., Russell, J.M., Huang, Y.S., Sinninghe Damst \acute{e} J.S., Hopmans, E.C., and Cohen, A.S.: Northern hemisphere controls on tropical southeast African climate during the past 60,000 years, *Science*, 322, 252-255, 2008.



- Veres, D., Bazin, L., Landais, A., Toy é Mahamadou, Kele, H., Lemieux-Dudon, B., Parrenin, F., Martinerie, P., Blayo, E., Blunier, T., Capron, E., Chappellaz, J., Rasmussen, S.O., Severi, M., Svensson, A., Vinther, B., and Wolff, E. W.: The Antarctic ice core chronology (AICC2012): An optimized multi-parameter and multi-site dating approach for the last 120 thousand years, *Clim. Past.*, 9, 1733-1748, 2013.
- 5 WAIS Divide Project Members.: Precise inter-polar phasing of abrupt climate change during the last ice age, *Nature*, 520, 661-665, 2015.
- Wang, Y., Cheng, H., Edwards, R.L., An, Z., Wu, J., Shen, C.-C., and Dorale, J.A.: A high-resolution absolute-dated late Pleistocene monsoon record from Hulu Cave, China, *Science*, 294, 2345-2348, 2001.
- Wang, Y., Cheng, H., Edwards, R.L., Kong, X., Shao, X., Chen, S., Wu, J., Jiang, X., and An, Z.: Millennial-and
10 orbital-scale changes in the East Asian monsoon over the past 224,000 years, *Nature*, 451, 1090-1093, 2008.
- Wolff, E.W., Chappellaz, J., Blunier, T., Rasmussen, S.O., and Svensson, A.: Millennial-scale variability during the last glacial: The ice core record, *Quat. Sci. Rev.*, 29, 2828-2838, 2010.
- Xia, Z., Kong, X., Jiang, X., and Cheng, H.: Precise dating of East-Asian-Monsoon D/O events during 95-56 ka BP: Based on stalagmite data from Shanbao Cave at Shennongjia, China, *Sci. China. Ser. D.*, 50, 228-235, 2007.
- 15 Yuan, D.X., Cheng, H., Edwards, R.L., Dykoski, C.A., Kelly, M.J., Zhang, M.L., Qing, J.M., Lin, Y.S., Wang, Y.J., Wu, J.Y., Dorale, J.A., An, Z.S., and Cai, Y.J.: Timing, duration, and transitions of the last interglacial Asian monsoon, *Science*, 304, 575-578, 2004.
- Zhang, W., Wu, J., Wang, Y., Wang, Y., Cheng, H., Kong, X., and Duan, F.: A detailed East Asian monsoon history surrounding the 'Mystery Interval' derived from three Chinese speleothem records, *Quat. Res.*, 82, 154-163, 2014.
- 20 Zhang, T.T., Li, T.Y., Cheng, H., Edwards, R.L., Shen, C.-C., Spötl, C., Li, H.C., Han, L.Y., Li, J.Y., Huang, C.X., and Zhao, X.: Stalagmite-inferred centennial variability of the Asian summer monsoon in southwest China between 58 and 79 ka, *Quat. Sci. Rev.*, 160, 1-12, 2017.
- Zhao, K., Wang, Y., Edwards, R.L., Cheng, H., and Liu, D.: High-resolution stalagmite $\delta^{18}\text{O}$ records of Asian monsoon changes in central and southern China spanning the MIS 3/2 transition, *Earth. Planet. Sci. Lett.*, 298, 191-198,
25 2010.
- Zhou, H.Y., Zhao, J.X., and Wang, Q.: Speleothem-derived Asian summer monsoon variations in Central China, 54-46 ka, *J. Quat. Sci.*, 26, 781-790, 2011.



Table 1. ^{230}Th dating results for stalagmites SX10 and SX16, Sanxing Cave, southwestern China. Corrected ^{230}Th ages are indicated in bold. Errors are 2σ analytical errors. Corrected ^{230}Th ages were calculated with an assumed initial $^{230}\text{Th}/^{232}\text{Th}$ atomic ratio of $(4\pm 2) \times 10^{-6}$.

Sample number	Depth (cm)	^{238}U (ng/g)	^{232}Th (pg/g)	$\delta^{234}\text{U}$ (measured)	$^{230}\text{Th}/^{238}\text{U}$ (activity)	$^{230}\text{Th}/^{232}\text{Th}$ (atomic ratio, $\times 10^{-6}$)	^{230}Th age (yr BP) (uncorrected)	^{230}Th age (yr BP) (corrected)	$^{234}\text{U}_{\text{Initial}}$ (corrected)
SX10-12	1.2	1764±1.7	217±8	2326±3	1.785±0.003	238977±8333	75807±196	75740±196	2881±4
SX10-45	4.5	1430±1.1	353±10	2322±2	1.784±0.003	119085±3230	75894±153	75827±153	2877±3
SX10-75	7.5	1667±1.4	510±9	2331±2	1.791±0.003	96580±1800	76009±168	75941±168	2889±3
SX10-125	12.5	1505±1.2	86±10	2322±2	1.787±0.003	513911±57439	76113±177	76047±177	2878±3
SX10-255	25.5	1366±1.3	406±9	2305±3	1.788±0.003	99196±2127	76681±168	76613±168	2862±4
SX10-335	33.5	1375±1.2	105±9	2301±2	1.792±0.002	387822±32044	77004±161	76937±161	2860±3
SX10-372	37.2	1787±1.7	112±11	2297±3	1.790±0.003	472015±44614	77058±198	76992±198	2855±4
SX10-435	43.5	1471±1.4	267±10	2303±3	1.797±0.003	163460±5879	77225±201	77158±201	2864±4
SX10-510	51.0	1637±2.5	156±8	2301±5	1.803±0.005	311675±15532	77664±308	77597±308	2865±7
SX10-620	62.0	1929±1.8	348±7	2288±3	1.803±0.003	164849±3327	78052±173	77984±173	2852±4
SX10-650	65.0	2031±2.1	93±7	2287±3	1.803±0.003	648541±51380	78087±192	78021±192	2851±4
SX10-694	69.4	1841±2.9	130±7	2292±5	1.807±0.004	420789±23497	78171±280	78105±280	2857±7
SX10-767	76.7	1832±2.5	133±8	2284±5	1.803±0.004	410012±24821	78222±283	78156±283	2848±6
SX10-807	80.7	1557±2.4	364±8	2287±5	1.808±0.004	127519±2909	78414±287	78347±287	2853±7
SX10-825	82.5	1759±1.9	261±9	2284±3	1.813±0.003	201309±6690	78745±209	78678±209	2853±5
SX10-995	99.5	1692±1.8	725±10	2281±4	1.815±0.003	69826±1010	79017±213	78949±213	2850±5
SX16-287	28.7	1872±2.0	2740±7	1895±3	1.436±0.003	16196±52	68836±225	68774±225	2302±4
SX16-300	30.0	756±1.0	1553±6	1913±5	1.556±0.004	12514±54	75838±321	75755±321	2370±6
SX16-352	35.2	546±1.0	653±9	1908±4	1.568±0.003	21591±294	76699±216	76623±216	2369±5
SX16-392	39.2	759±1.0	4420±11	1891±4	1.564±0.003	4430±13	77113±269	77001±270	2351±5

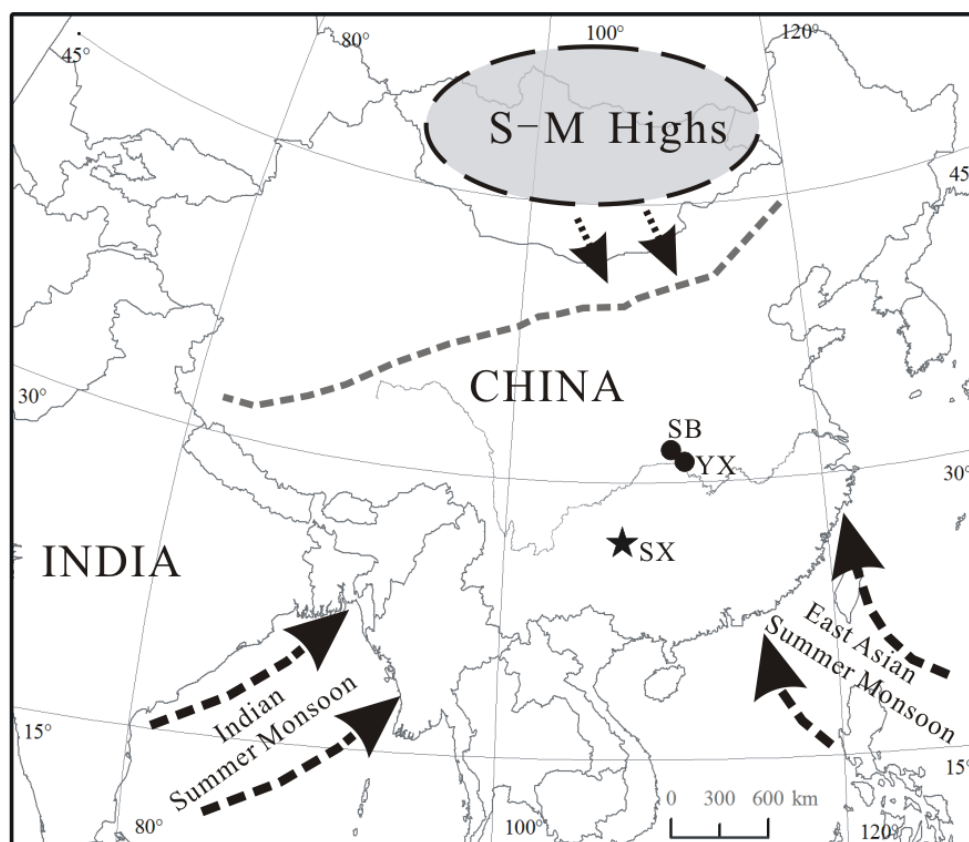


Fig. 1. A map of ASM territory with locations of Sanbao (SB) Cave (Wang et al., 2008); Yongxing (YX) Cave (Chen et al., 2016) and Sanxing (SX) Cave (this study). Dashed line represents the average modern ASM limit. The elliptical area denotes the position of the Siberian-Mongolian Highs (S-M Highs).

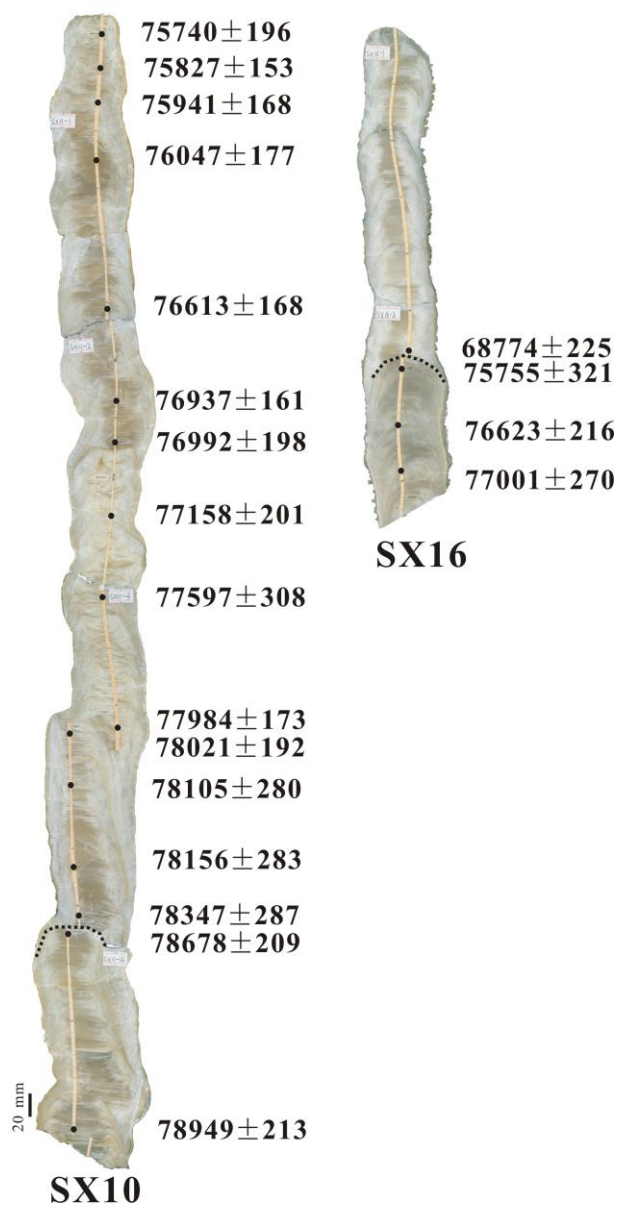


Fig. 2. Photographs of two stalagmites SX10 and SX16 collected from Sanxing Cave. Black dots indicate the layers for U-Th dating and the determined ages (yr BP) are listed on the right-hand side. Black dashed lines denote hiatuses. Subsamples for $\delta^{18}\text{O}$ analysis were drilled along light brown lines.

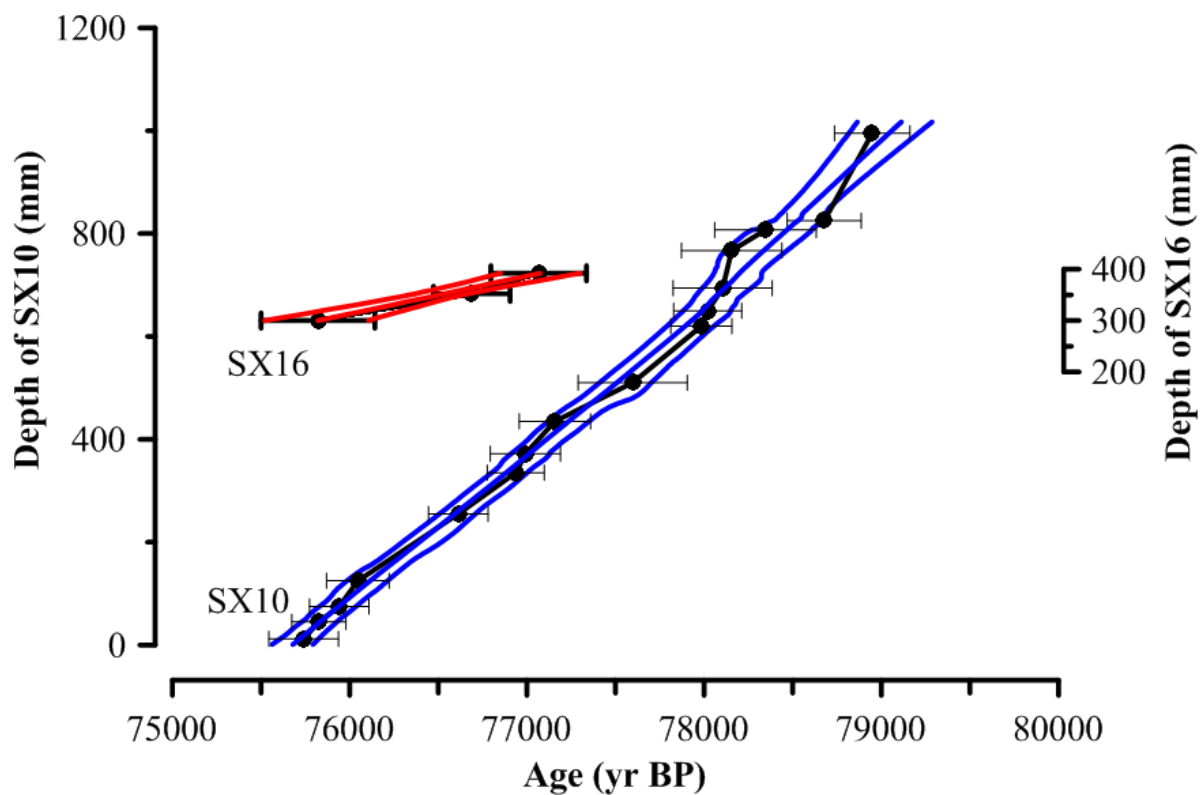


Fig. 3. Chronologies for stalagmites SX10 and SX16 using a linear interpolation method (black) and StalAge model with 95% confidence interval (Scholz and Hoffmann, 2011).

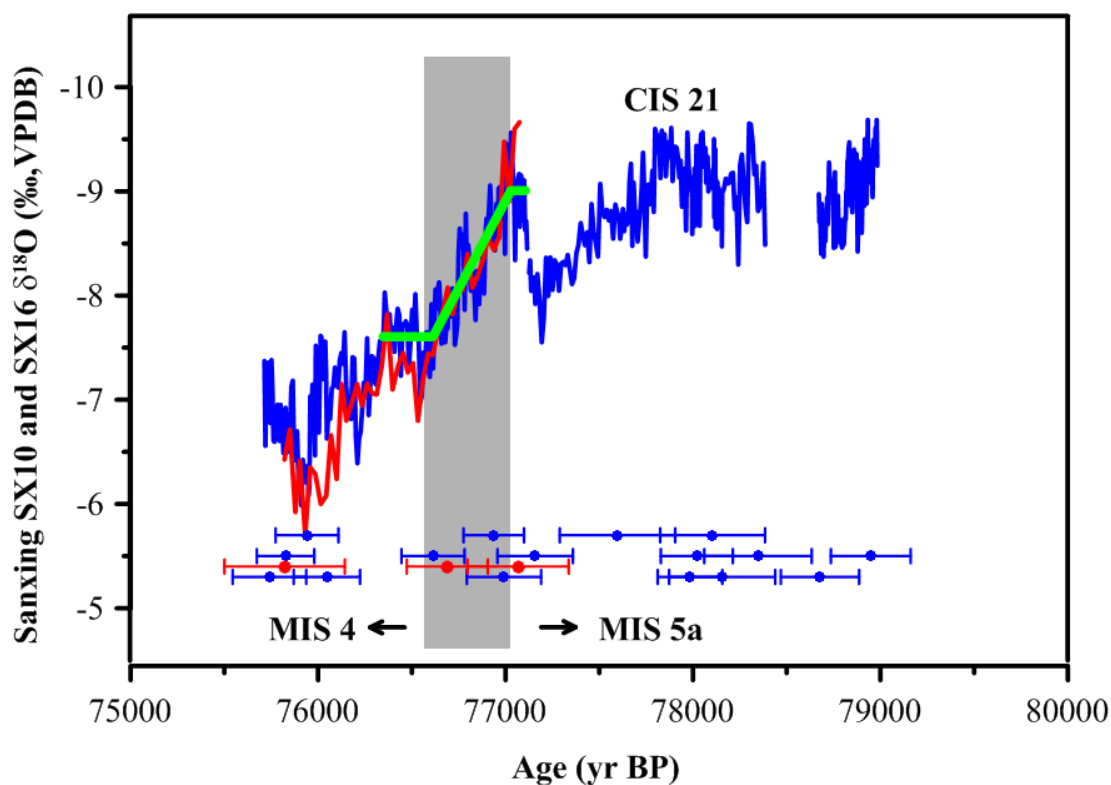


Fig. 4. $\delta^{18}\text{O}$ time series of stalagmites SX10 (blue) and SX16 (red). Green polyline is the ramp (Mudelsee, 2000) of SX 10 $\delta^{18}\text{O}$ record. MIS substages 5a and 4 are given at bottom, separated by a vertical gray bar. ^{230}Th ages and errors are color-coded by stalagmites.

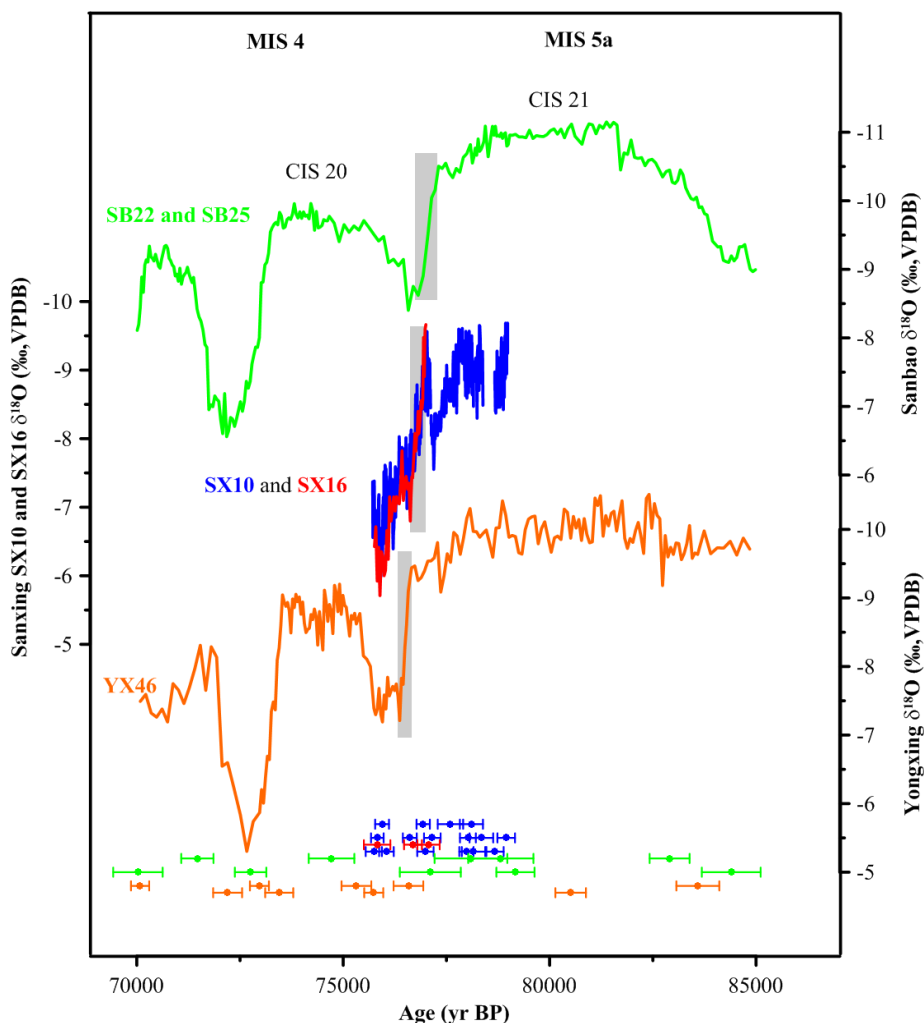


Fig. 5. Comparison of $\delta^{18}\text{O}$ time series of stalagmites SX10 (blue) and SX16 (red) with Sanbao SB22 and SB25 (green) (Wang et al., 2008), and Yongxing YX46 (orange) (Chen et al., 2016). MIS substages 5a and 4 are given at top. Vertical bars denote the transition of CIS 21 termination. ^{230}Th ages and errors are color-coded by stalagmite.

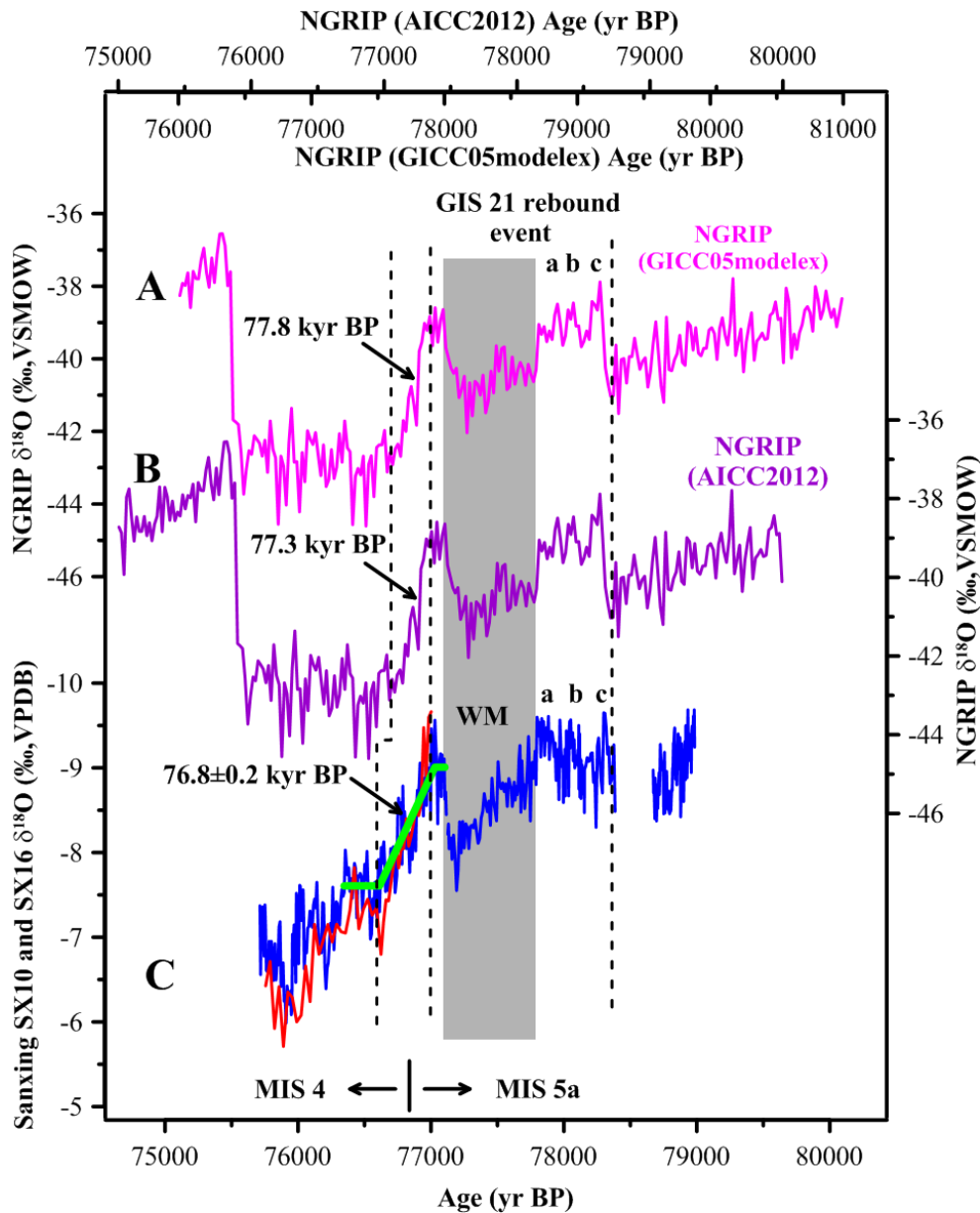


Fig.6. Comparison of $\delta^{18}\text{O}$ records between Sanxing Cave and NGRIP ice core during 81-75 kyr BP. NGRIP record on timescales of (A) GICC05modelext (pink, Wolff et al., 2010), and (B) AICC2012 (purple, Veres et al., 2013). (C) Sanxing $\delta^{18}\text{O}$ record. Gray bar denotes the weak monsoon event (WM) within CIS 21 rebound event. Three letters of **a**, **b**, and **c** indicate the strong monsoon events during CIS 21 rebound event. Green polyline is the ramp of SX10 $\delta^{18}\text{O}$ record. MIS substages 5a and 4 are given at bottom.